Experimental Verification of Frequency Mappings with Hadamard Transform for Power Line Communications Channel

T. Lukusa, K. Ouahada, A. R. Ndjiongue, H. C. Ferreira and A. J. Han Vinck‡
Department of Electric and Electronic Engineering Science, University of Johannesburg, South Africa
‡ Institute for Experimental Mathematics, Essen, Germany
Email: {tedym, kouahada, alainn, hcferreira}@uj.ac.za, han.vinck@uni-due.de

***Abstract*— In recent years, given the prominence of the electrical distribution network, power line communications channel has drawn interests among researchers throughout the globe. *M*-ary FSK modulation scheme has been extensively used when combined with certain error correcting codes because of its viability and robustness over the power line communications channel.**

In this paper, we make use of the sign changes property in the Hadamard transform combined together with convolutional codes and *M*-ary FSK modulation scheme to experimentally use the technique of "frequency mappings" in a real power line environment.

Interesting experimental results show that this technique is very useful without the need of combining coding techniques and modulations that is usually based on the combination of convolutional codes and *M*-FSK modulation schemes.

I. Introduction

Hadamard transform is considered as the simplest of the usual orthogonal transform like the Fourier transform. Hadamard matrices have been used successfully in different applications such as switching networks [1], error-correcting codes and signal processing [2], [3].

Distance-preserving mapping (DPM) techniques have shown their viability when combined with M-FSK modulation to combat certain noise in power line communications channel. This was proved through simulation results. More often, designing a distance preserving mapping codes with desired or predictable properties, in terms of Hamming distance, demands construction algorithms which may be difficult and complex to construct. However, authors in [4], suggested the use of Hadamard transform properties to circumvent the need for specific constructions and complicated algorithms.

This present paper proposes the investigation of the performance of the frequency mappings technique, which results from arranging non-binary symbols based on certain properties of the Hadamard transform in real time over power line channel. Furthermore a customized experimental platform was constructed in order to gain more control on the transmission of data during the experimentation phase.

The paper is arranged as follow. In Section II we present frequency mapping technique and we show how the property of Hadamard matrix is used to accomplish the frequency mapping.

In Section III, we present the communication system in which we also show through functional diagram how the implementation of frequency mapping is accomplished.

Then we proceed with the hardware implementation in Section IV. Section V presents the results collected from the experimental set-up. Finally a conclusion is provided in Section VI regarding the work presented in this paper.

II. Frequency Mapping Technique

A. Hadmard Matrix Definition

Here we introduce a mathematical definition of Hadamard transform as presented in [6]. The Hadamard matrix is formed out of the projection onto a set of Walsh functions and in such a way that distinct rows or columns form an orthogonal basis.

The Hadamard matrix H_1 is defined as:

$$H_1 = \frac{1}{\sqrt{2}} \begin{bmatrix} +1 & +1 \\ +1 & -1 \end{bmatrix}, \tag{1}$$

and by using the Kronecker product of two matrices, the Hadamard matrix H_n of order 2^n is defined recursively by:

$$H_n = H_1 \otimes H_{n-1} = \begin{bmatrix} +H_{n-1} & +H_{n-1} \\ +H_{n-1} & -H_{n-1} \end{bmatrix}. \tag{2}$$

Example 1 For $n = 2$ and $n = 3$, we have:

$$H_2 = \frac{1}{2} \begin{bmatrix} +1 & +1 & +1 & +1 \\ +1 & -1 & +1 & -1 \\ +1 & +1 & -1 & -1 \\ +1 & -1 & -1 & +1 \end{bmatrix},$$

$$H_3 = \frac{1}{2\sqrt{2}} \begin{bmatrix} +1 & +1 & +1 & +1 & +1 & +1 & +1 & +1 \\ +1 & -1 & +1 & -1 & +1 & -1 & +1 & -1 \\ +1 & +1 & -1 & -1 & +1 & +1 & -1 & -1 \\ +1 & -1 & -1 & +1 & +1 & -1 & -1 & +1 \\ +1 & +1 & +1 & +1 & -1 & -1 & -1 & -1 \\ +1 & -1 & +1 & -1 & -1 & +1 & -1 & +1 \\ +1 & +1 & -1 & -1 & -1 & -1 & +1 & +1 \\ +1 & -1 & -1 & +1 & -1 & +1 & +1 & -1 \end{bmatrix}. \quad \square$$

B. Frequency Mapping Concept

In this subsection, we briefly present a concept of frequency mapping as in [7]. The rows of Hadamard matrix, which represent the amplitudes of Walsh functions on the interval [0 1], show sign changes also referred to as sequency. Now, since frequency is intuitively related to the rate of change of a periodical signal, a sequency (number of sign change) can be thought, to some extent, as representing the frequency of non-periodical signal. Therefore, there is a certain correspondence, in a proportional way, between the number of sign changes and frequencies.

Example 2 For $n = 2$

For the case of $n = 2$, we have four rows in our Hadamard matrix as presented in Fig. 1. It is clear from the sequency represented by numbers in the column presented and in the form of a set $\{0, 3, 1, 2\}$, are actually the numbers of zero–crossings or sign changes in each row.

Having done the above and now taking advantage of the fact that since the Hadamard matrix dimension is given by $2^n \times 2^n$; it becomes easy to use *M*-FSK signaling [8], [9] since $M = 2^n$. As in [4], the start frequency, shown in Example 2, is directly proportional to the notation index which represents the number of sign changes. The rows in a Hadamard matrix represent the Walsh functions, which are defined as follows:

$$W(k,t) = \prod_{i=0}^{r-1} Sign[\cos^{k_i}(2^i\pi)t] \tag{3}$$

where $r = \lfloor (log_2(k) + 1) \rfloor$, k is the index of Walsh function, k_i is the i^{th} bit of k in binary.

If we consider that Walsh-functions consist of trains of square pulses, then we can introduce the concept of sign change in each Walsh function [5]. The number of sign changes in a row of a Hadamard matrix is called sequency.

As it is known that Walsh-Hadamard matrix is constructed from the Hadamard matrix itself by just rearranging the order of the rows of the matrix taking into consideration the number of sign changes in each corresponding Walsh functions. Since we are interested only in the number of sign changes, we will focus only in the rest of the paper on the Hadamard matrices.

Therefore, in order to produce frequency sequences or frequency based permutation sequences, each start frequency is followed by the $M - 1$ remaining frequencies in an ascending and cyclic way as shown in Fig.2. Thus, for instance, if the starting frequency, for $M = 4$, is f_3 the following $M - 1$ frequencies are $f_0, f_1$and f_2 which effectively results into frequency sequence$f_3 f_0 f_1 f_2$. □

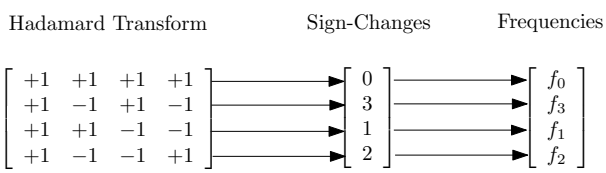

Fig. 1. Hadamard matrix and sign changes: $M = 4$

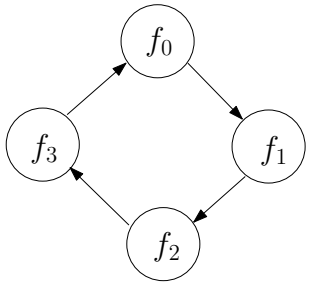

Fig. 2. Cyclic Frequency-shift Diagram

III. Communication System

A. Transmitter Functional Role

As shown in Fig. 3, convolutional outputs data are generated to be sent over the channel. These codes are used to gain advantage of the Viterbi decoding algorithm. Since Hadamard matrix and sign changes are used in the communication system, it is important to select the convolutional codes rate and constraint length so as to suit the Hadamard matrix dimensions. Therefore since we desire a simple communication system, a second order Hadamard matrix and a convolutional codes with rate $R = 1/2$ and constraint length $K = 3$ can be easily selected. Subsequently we have then accomplished our goal to map the convolutional codes outputs to the rows of the Hadamard matrix.

On the implementation level, the sign change as briefly mentioned in the previous section, is used, in the software environment, to select the first starting frequency and implements the cyclic shift of the M-ary FSK frequencies.

B. Receiver functional role

Since we introduced sign change as our main concept to undo the importance mapping, it is then equally important to re-introduce this concept in the decoding process.

As shown in Fig. 4, frequency mapping have been successfully integrated in the state diagram, and subsequently, the trellis diagram, structure of the convolutional codes. It

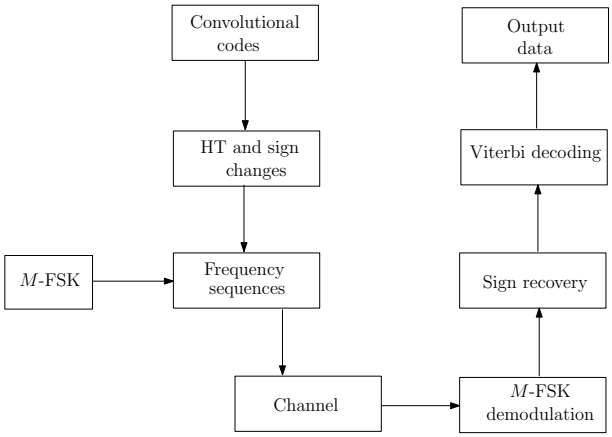

Fig. 3. Communication system

becomes then very intuitive to use a sign recovery mechanism based on the frequency sequences received and then implement a Viterbi algorithm [10], as shown in Fig. 3, to get back the transmitted data.

IV. Hardware Verification

A. Hardware Description

- The transmitter modules consist of a personal computer (PC A) and customized electronic circuit in which a PIC16F887 can be found. The PIC16F887 implements the cyclic shift to produce the desired frequency sequences. In effect, four pins were configured and directly connected to the four sine wave generator ICs (XR2206CP). The communication between the PIC16F887 and the personal computer was accomplished via serial linked since both the PIC and personal computer have such capability. Data are Matlab generated in conjunction the RS232 standards.
- The serial communication thus implemented could only achieve 2000 bps. Any transmission speed beyond or below 2000 bps resulted in wrong data being transmitted. Furthermore, the sine wave generators where tuned to frequencies: $f_0 = 75KHz$, $f_1 = 85KHz$, $f_2 = 100KHz$, $f_3 = 120KHz$.
  Which are within CENELEC bands [11], [13]. As it can be noticed, the frequencies were selected throughout the CENELEC band due to the poor frequency discrimination capability of the receiver.
- The receiver modules consist of a personal computer (PC B) and a customized electronic circuit and a PIC16F887. Similar to the transmitter, the serial communication were also implemented for the same reasons as previously stated. In order to maintain synchronization throughout the entire communication system, a communication speed of 2000 bps was set. The detection was only accomplished through LM 567 ICs which are widely used in tone detection circuits.

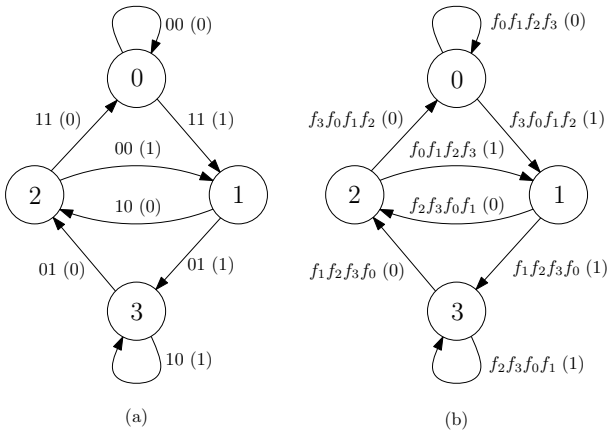

Fig. 4. Frequency mapping on convolutional state diagram

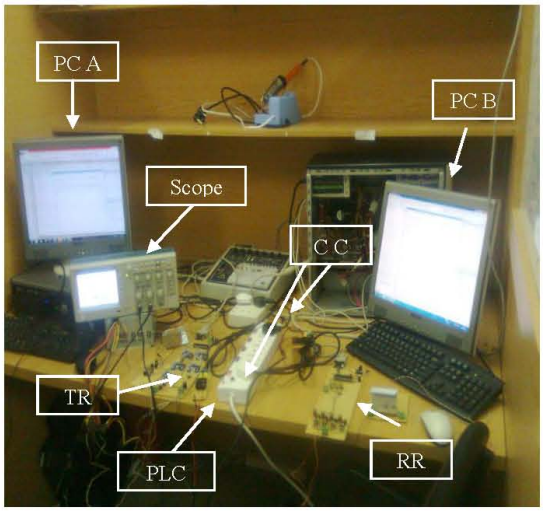

Fig. 5. Experimental setup

B. Experimental Setup description

The experimental setup is as represented in Fig. 5. The power line channel (PLC) is a single phase of the three phase electrical network of the laboratory. The personal computers (PC A and PC B), DC power source were supplied on the electrical network phase. The coupling circuits (CC), of the communication system, were plugged on a different phase of the electrical network. This was accomplished to mitigate noise contributions from the DC sources as well as those from the personal computers.

As clearly shown in Fig. 6, the objective of this experiment is to communicate over the power line channel. In essence computer A, through MATLAB, generates binary data which are then frequency mapped and sent over the power line channel via coupling circuits. Computer B performs sign recovery and eventually data is recovered with more or less corruption depending on the communication signal strength and the presence of noise in the channel.

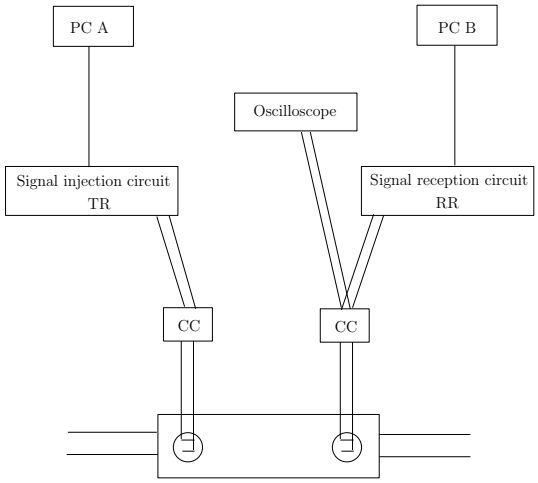

Fig. 6. Experimental setup synopsis

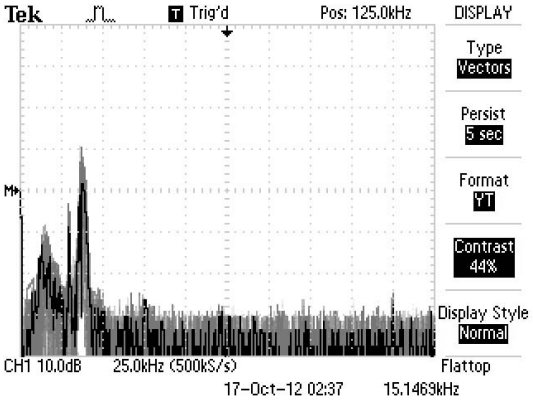

Fig. 7. Background Noise

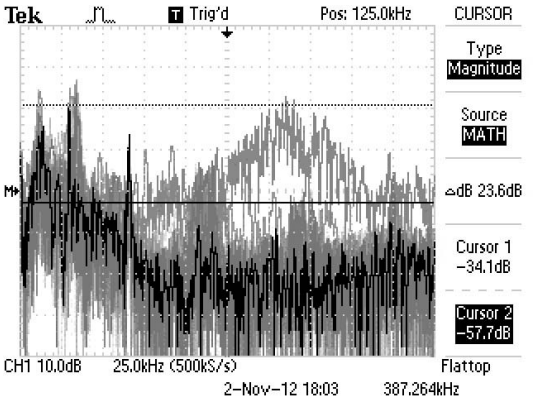

Fig. 8. Impulse Noise Burst

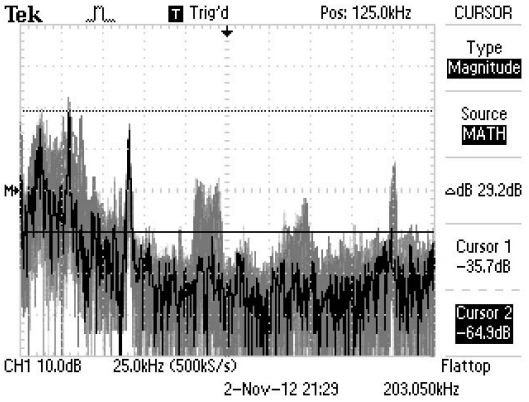

Fig. 9. Narrowband Noise

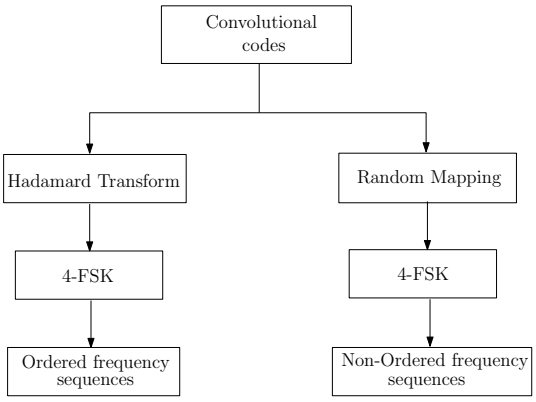

Fig. 10. Process for generating frequency sequences

C. Power Line Channel

Power line channel is manly characterized by the noise disturbances the presence of which makes the communication very challenging. Three main types of noise, background noise, narrowband noise and impulse noise, observed during this experimentation.

Background noise [12] covers the entire CENELEC band and in reality it extends beyond the CENELEC spectrum region. It is easily identifiable due to its flattened profile as frequency increases. Fig. 7 was captured when the activity in the laboratory was at the lowest level i.e. between 4 a.m. and 7 a.m.

For frequencies below $40KHz$, the average noise power is $-38.8dBV_{rms}$ $(3mV_{rms})$ while for frequencies above $40KHz$, the average noise power is $-66dBV_{rms}$ $(0.065mV_{rms})$, which is mostly in the form of a background noise. The spectrum region below $40KHz$ presents some challenges for transmitting communication signal through the channel. Consequently the spectrum region above $40kHz$ is favorable for implementing power line communications

Impulse noise [12], [14] is clearly illustrated in Fig. 8 and was captured between 8 a.m. and 1 p.m. As shown in Fig. 8, this noise easily inflates the noise level and can cover a wide range of frequency. Its occurrence is sporadic therefore a frequency and time diversities needs to be implemented to combat it.

In Fig. 9, we clearly indicate the narrowband noise. We especially noticed a permanent peak at $65KHz$, which seemed to strengthen between 8 a.m. and 6 p.m.

V. Experimental Setup Description

Power line channel (PLC) is a single phase of the three phase electrical network of the laboratory. The personal computers (PC A and PC B), DC power source were supplied on the electrical network phase. The coupling circuits (CC), of the communication system, were plugged on a different phase of the electrical network. This was accomplished to mitigate noise contributions from the DC sources as well as those from the personal computers.

The objective of this experiment is to communicate over the power line channel [12]. In essence computer A, through MATLAB, generates binary data which are then frequency mapped and sent over the power line channel via coupling circuits. Computer B performs sign recovery and eventually data is recovered with more or less corruption depending on the communication signal strength and the presence of noise in the channel.

VI. Experimental results

Both the transmitter and receiver coupling circuits were plugged on the same electrical network phase. The receiver

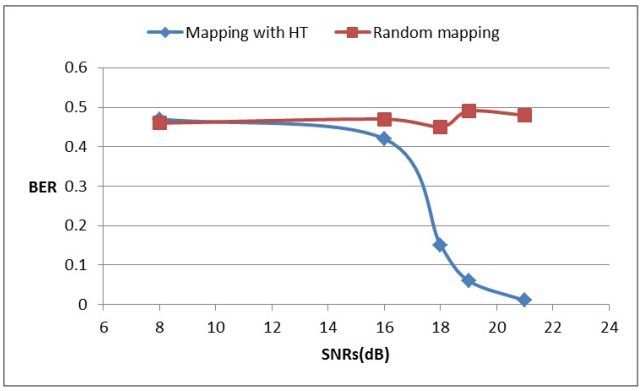

Fig. 11. BER vs. SNRs (symbol energy to noise ratio)

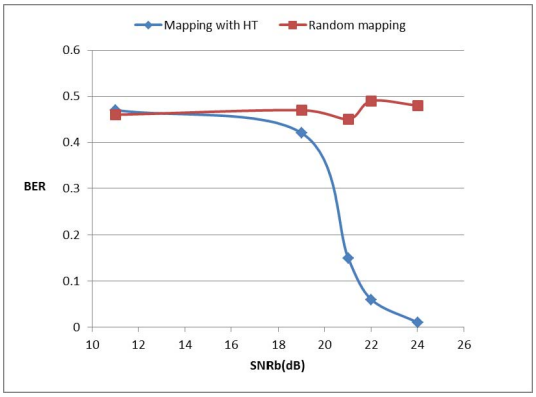

Fig. 12. BER vs. SNRb (bit energy to noise ratio)

and the transmitter plugs were about 10 cm apart to avoid weakening the communication signal strength.

In order to investigate the performance of the Hadamard transform frequency mapping technique, we compared the performance of randomly generated mapping with the Hadamard transform [4] frequency mapping as describe in Fig. 10.

The performance test was conducted during daytime where the laboratory activity showed the average noise level well around the values described previously. As shown in Fig. 11, the SNRs, between $8dB$ and $21dB$, required for the communication to take place was well above the noise level floor, which was considered to be around $-36dB$. Here the SNRs represents the energy per symbol as observed on the oscilloscope. Since we know that for every two bits, we transmit four signals or symbols, therefore the SNR bit or SNRb can be expressed as:

$$\begin{aligned} SNRb &= 10log_{10}((log_2 M) \times 10^{\frac{SNRs}{10}}) \\ &= 10log_{10}(2 \times 10^{\frac{SNRs}{10}}) \end{aligned} \tag{4}$$

Fig. 11 gives the performance based on the energy per symbol SNRs since our observation is solely based on a direct measurement from the oscilloscope. However, we should not that we could only observe one symbol at a time during transmission, therefore, according to the previous formula; we actually spent much more energy during transmission than what Fig. 11 suggests. Thus Fig. 12 gives a true reflection of the performance of the system as the SNR is expressed as the amount of bit energy per noise power or SNRb.

The maximum signal used during the experiment was measured around $-15dB(178mV_{rms})$, still within the CENELEC requirements. Furthermore, the results were obtained by sending data packet of length 100 bits over the channel to accommodate the memory limits of the communication system, and therefore resulting in the low BER as observed in Fig. 11.

From the curves in Fig. 12, we observe for low SNR values (below 15 dB), both the Hadamard mapped data and the Random mapped data, equally performed in terms of BER. It is only when we tend to reach a free channel SNR condition (high SNR values), Hadamard mapped data BER performance improve significantly as the SNRs or SNRb increases.

The high SNR values observed during this experimentation are indicative of flaws in the design of the communication system. We can attribute these (high SNR values) to the threshold detection level required at the receiver, which was observed to be around, and to the copper wires that were used on the verroboard as well as to connect different the components of the system.

VII. Conclusion

Distance preserving mappings usually necessitate a construction algorithm. The aim of construction algorithms is to select the right permutation sequences yielding to better performance. However in this paper, through taking benefit of the property of Hadamard transform, we ordered frequency sequences which yield better performance when compared with randomly arranged frequency sequences.

The results obtained in this experimentation need some improvement through using very well designed platform. Since the main processor is microcontroller, a higher performant processor with a better memory capacity can also be considered.

References

[1] R. T. Chien, "A class of optimum noiseless load-sharing matrix switches," *IBM J. Res. Develop.*, vol. 4, pp. 414–417, 1960.

[2] W. K. Pratt, J. Kane, and H. C. Andrews, "Hadamard transform image coding," *Proc. IEEE*, vol. 57, pp. 58–68, 1969.

[3] J. E. Whelchel and D. F. Guinn, "The Fast Fourier-Hadamard transform and its use in signal representation and classification," *1968 EASCOM Rec.*, pp. 561–573.

[4] M.T. Lukusa, K. Ouahada, H.C. Ferreira, "Frequency Mappings with Hadamard Transform for Power Line Communications Channel", IEEE International Symposium on Power-line communication theory and its applications 2011,pp.418-423.J. Clerk Maxwell, A Treatise on Electricity and Magnetism, 3rd ed., vol. 2. Oxford: Clarendon, 1892, pp.68-73.

[5] N. M. Blackman, "Some Comments Concerning Walsh Functions," submitted to *IEEE Transaction on Information Theory*, May 1972.

[6] K. J. Horadam, "Hadamard Matrices and their applications". Princeton University Press, New Jersey, 2007.K. Elissa, "Title of paper if known," unpublished.

[7] N. M. Blackman,"Some Comments Concerning Walsh Functions," submitted to IEEE transaction on Information Theory, May 1972.

[8] F. G. Stremler, Introduction to Communication Systems. 2nd edition, Addison -Wesley Publishing Company, Canada, 1982.

[9] Simon Haykin, Communication Systems. 4th edition, John Wiley Sons, Inc., New York, 2001.
[10] A. Viterbi and J. Omura, Principles of Digital Communication and Coding. McGraw-Hill Kogakusha LTD, Tokyo Japan, 1979.
[11] M. Gebhardt, F. Weinmann, K. Dostert, "Physical and Regulatory Constraints for Communication over the Power Supply Grid", IEEE Commu.Mag., vol. 41, pp.84-90, May 2003.M. Young, The Technical Writer's Handbook. Mill Valley, CA: University Science, 1989.
[12] K. Dostert, Powerline communications, Prentice-Hall, 2001.
[13] "CENELEC"Available:http://www.cenelec.eu/Cenelec/Homepage.htm, October 11th, 2011.
[14] M. Gotz, M.Rapp, K. Dostert,"Power Line Channel Charcteristics and Their Effect on Communication System Design," IEEE Commu.Mag., vol. 42, pp.78-86, April 2004.